

# Duplex Formation at the 5' End Affects the Quadruplex Conformation of the Human Telomeric Repeat Overhang in Sodium but Not in Potassium<sup>†</sup>

Timur I. Gaynutdinov,<sup>‡</sup> Patrick Brown,<sup>§</sup> Ronald D. Neumann,<sup>‡</sup> and Igor G. Panyutin<sup>\*‡</sup>

<sup>‡</sup>*Department of Radiology and Imaging Sciences, Clinical Center, National Institutes of Health, Bethesda, Maryland 20892-1180, and*

<sup>§</sup>*Dynamics of Macromolecular Assembly, Laboratory of Bioengineering and Physical Science, National Institute of Biomedical Imaging and Bioengineering, National Institutes of Health, Bethesda, Maryland 20892-1180*

*Received June 23, 2009; Revised Manuscript Received October 20, 2009*

**ABSTRACT:** Human telomeres contain numerous copies of the (TTAGGG)<sub>n</sub>·(AATCCC)<sub>n</sub> repeated sequence with multiple TTAGGG repeats in 3' single-stranded overhangs. Single-stranded oligonucleotides consisting of four TTAGGG repeats can fold into various intramolecular quadruplex structures stabilized by quartets of guanines. The quadruplex structures are believed to play a role in telomere functions and considered as targets for anticancer drug design. In an effort to create a more realistic model of telomeric DNA, we designed oligonucleotides containing a duplex region at the 5' end and four telomeric repeats in the 3' overhang. We applied CD spectroscopy and <sup>125</sup>I radioprobng to determine the conformation of the quadruplexes formed in the 3' overhangs. We found that in the presence of NaCl the conformation of the quadruplex changes with formation of the 5' duplex and depends on the position of the interface between the duplex and the 3' telomeric sequence. When the duplex region extended to the first T of the first TTAGGG repeat, both CD and radioprobng data are consistent with the parallel propeller conformation of the overhang. In the presence of KCl, formation of the duplex at the 5' end of DNA molecules did not change the fold of the quadruplex in the overhang which was interpreted as a mixture of two isomers of 3+1 conformation regardless of the duplex–overhang interface position. Our results demonstrate that the interface between the duplex and single-stranded overhang can affect the conformation of the telomeric quadruplex.

At the ends of eukaryotic chromosomes are often found repeated sequences containing stretches of guanines; for example, all mammalian telomeres contain numerous (TTAGGG)<sub>n</sub>·(AATCCC)<sub>n</sub> repeats with multiple TTAGGG repeats in the 3' single-stranded overhangs (1, 2). The exact mechanism of function of these sequences is still unclear, but they all have a common feature: a single-stranded G-rich strand can form a quadruplex structure that is stabilized by hydrogen bonds between four guanines forming a G-tetrad (3–6). To form an intramolecular quadruplex, a human telomeric sequence must contain at least four runs of guanines, i.e., AGGG(TTAGGG)<sub>3</sub>. Most of the data on the structure of telomeric DNA were obtained by studying conformations of such “minimal” G-quadruplex-forming telomeric oligonucleotides (7–10). It was found that these oligonucleotides could adopt a variety of quadruplex conformations that can be broadly divided into parallel, antiparallel, and mixed types depending on the relative orientation of the neighboring runs of guanines. Within these broad classes, there are a variety of folds differing by the conformations of the TTA connecting loops. Some of the quadruplex conformations are shown in Figure 1.

The fold of the telomeric oligonucleotide depends on the type of stabilizing monovalent ions (9, 11–13), and on the flanking nucleotides that can interact with the loops of the quadruplex,

thus stabilizing a particular conformation (9, 10, 14–16). Some of the conformations were implicated in the compaction of the telomeric DNA (8, 9) and, thus, in protection of the ends of the chromosomes. For example, in the all-parallel, so-called propeller conformation (8) and in the so-called 3+1 conformation (9, 10), neighboring quadruplexes could stack to each other forming a well-compacted structure.

It is not clear if the structural polymorphism of the telomeric DNA has a biological role. To address this question, it is important to determine what conformation(s) the telomeric repeats adopt inside cells. This information would also help in the design of G-quadruplex binding drugs developed for anti-cancer activities by virtue of inhibiting the function of telomeres (reviewed in refs 17 and 18). In an attempt to create a more realistic model of the telomeric DNA, we designed DNA molecules containing a 5' duplex region and G-quadruplex-forming telomeric sequence at the 3' end. We first characterized the general type of G-quadruplex conformation of the molecules by CD<sup>1</sup> spectroscopy. We then applied <sup>125</sup>I radioprobng to determine the exact folding of the quadruplexes in these molecules. [<sup>125</sup>I]IdC (<sup>125</sup>I-dC) was incorporated at the 3' end of the telomeric repeats. Decay of <sup>125</sup>I produced DNA strand breaks in a distance-dependent manner, allowing us to determine the changes in folding of the G-quadruplex. We found that in the presence of Na<sup>+</sup> the conformation of the quadruplex dramatically changed upon 5' duplex formation and depended on the

<sup>†</sup>This research was supported by the Intramural Research Program of the National Institutes of Health, Clinical Center, and the National Institute of Biomedical Imaging and Bioengineering.

<sup>\*</sup>To whom correspondence should be addressed: NIH/CC/RAD&IS, Bldg. 10, Rm. 1C401, Bethesda, MD 20892-1180. E-mail: igorp@helix.nih.gov. Telephone: (301) 496-8308. Fax: (301) 480-9712.

<sup>1</sup>Abbreviations: ODN, oligodeoxyribonucleotide; T4 PNK, T4 polynucleotide kinase; PDB, Protein Data Bank; CD, circular dichroism; PAGE, polyacrylamide gel electrophoresis.

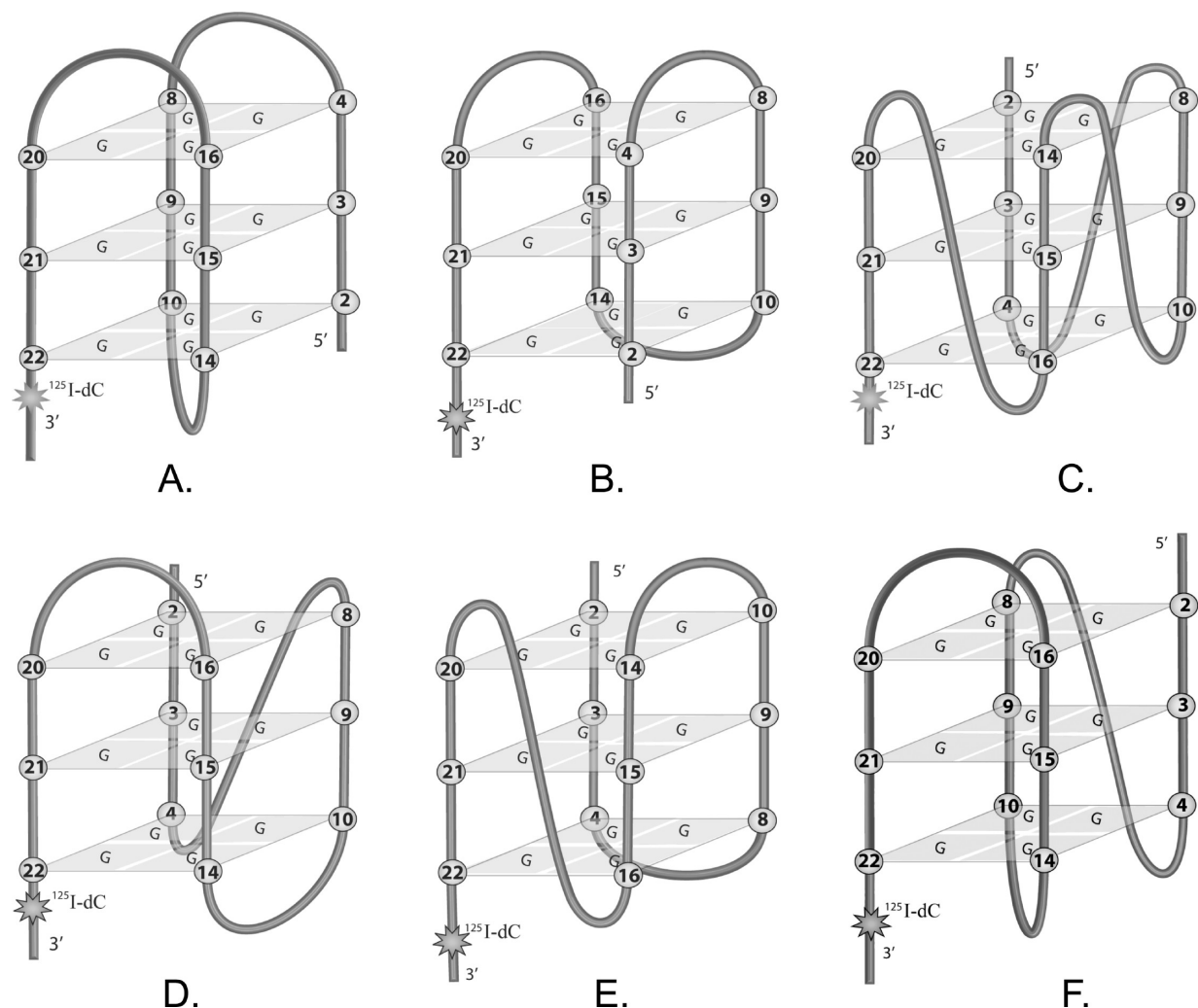


FIGURE 1: Schematic diagrams of possible intramolecular conformations of human telomeric quadruplexes. Antiparallel: (A) basket (G22†G20, G16†G14, G10†G8, G4†G2) and (B) chair (G22†G20, G16†G14, G10†G8, G4†G2). Parallel: (C) propeller (G22†G20, G16†G14, G10†G8, G4†G2). Mixed 3+1: (D) type I (G22†G20, G16†G14, G10†G8, G4†G2), (E) type II (G22†G20, G16†G14, G10†G8, G4†G2), and (F) 3+1 basket (G22†G20, G16†G14, G10†G8, G4†G2).

position of the duplex–overhang interface. In contrast, in the presence of  $K^+$ , the folding of the quadruplex was not affected by either the addition of the duplex or the position of the duplex–overhang interface.

## MATERIALS AND METHODS

**Oligodeoxyribonucleotides and Reagents.** All oligodeoxyribonucleotides (ODNs) (Table 1) were synthesized on an ABI394 DNA synthesizer (Applied Biosystems, Foster City, CA) and purified by denaturing polyacrylamide gel electrophoresis (PAGE) as described in detail in ref 11. The concentration of single-stranded ODN was measured at 260 nm on an Agilent 8453 diode array spectrophotometer and was calculated with the extinction coefficient calculator software (<http://www.basic.northwestern.edu/biotools/oligocalc.html>).

**Labeling and Purification of Oligodeoxyribonucleotides.** The telomeric ODNs were labeled with  $^{125}I$  using [ $^{125}I$ ]IdCTP (Perkin-Elmer, Waltham, MA) and Klenow fragment of DNA polymerase I (Fermentas, Hanover, MD) by the primer extension reaction (19). Primer and template oligonucleotides [T2 and T3 (Table 1)] were annealed by incubation for 40 min at 37 °C in Klenow buffer (Fermentas), in total amount of 20 pmol each in a final volume of 10  $\mu$ L. Then the whole sample was transferred to

the tube containing 77 pmol (170  $\mu$ Ci) of lyophilized [ $^{125}I$ ]IdCTP. The labeling reaction was initiated by addition of 0.5  $\mu$ L (5 units) of Klenow fragment of DNA polymerase I. After 5 min at room temperature, 1  $\mu$ L of a 1 mM dTTP solution was added and the reaction continued for an additional 2 min. The reaction was stopped by addition of 20  $\mu$ L of 10 mM EDTA; the mixture was extracted once with a phenol/chloroform mixture, and the product was purified by gel filtration on a MicroSpin G50 TE equilibrated column (GE Healthcare, Piscataway, NJ) and vacuum-dried. The resulting  $^{125}I$ -labeled oligonucleotide was dissolved in 1 $\times$  reaction buffer A (Fermentas) in the presence of 30 pmol (150  $\mu$ Ci) of [ $\gamma$ - $^{32}P$ ]ATP (Perkin-Elmer) and 10 units of T4 PNK (Fermentas) and incubated at 37 °C for 40 min. The resulting 5'- $^{32}P$ -labeled oligonucleotide was extracted with a phenol/chloroform mixture, purified by gel filtration on a MicroSpin G25 water equilibrated column (GE Healthcare), lyophilized, dissolved in 5  $\mu$ L of formamide stop solution (USB Corp., Cleveland, OH), and loaded onto a 6% denaturing PAGE gel. The band corresponding to the  $^{125}I$ - and  $^{32}P$ -labeled telomeric oligonucleotide was excised and eluted from the crushed gel with 100  $\mu$ L of 1 $\times$  TBS for 1 h on a shaking platform at room temperature. The sample was purified from acrylamide debris on a 0.22  $\mu$ m cellulose acetate X-spin filter (Corning Inc., Corning, NY),

Table 1: Oligonucleotides Used in This Study<sup>a</sup>

<b>T1</b>	5' - <sup>32</sup> P - GAGAACAGTCAACATACAGTGT <sub>1</sub> A <sub>1</sub> G <sub>2</sub> G <sub>3</sub> G <sub>4</sub> T <sub>5</sub> T <sub>6</sub> A <sub>7</sub> G <sub>8</sub> G <sub>9</sub> G <sub>10</sub> T <sub>11</sub> T <sub>12</sub> A <sub>13</sub> G <sub>14</sub> G <sub>15</sub> G <sub>16</sub> T <sub>17</sub> T <sub>18</sub> A <sub>19</sub> G <sub>20</sub> G <sub>21</sub> G <sub>22</sub> C* <sub>23</sub> T <sub>24</sub>	
Oligonucleotides used for <sup>125</sup> I-labeling of T1		
<b>T2</b>	5' - GAGAACAGTCAACATACAGTGTAGGGTTAGGGTTAGGGTTAGGG	Primer
<b>T3</b>	3' - TGTATGTCACAATCCCAATCCCAATCCCAATCCCGA	Complementary template
Complementary oligonucleotide complexes		
<b>TD1</b>	5' - <sup>32</sup> P - GAGAACAGTCAACATACAGTGTAGGGTTAGGGTTAGGGTTAGGGC*T	<b>T1</b>
	3' - CTCTTGTCAGTTGTATGTCACAAT	<b>T4</b>
<b>TD2</b>	5' - <sup>32</sup> P - GAGAACAGTCAACATACAGTGTAGGGTTAGGGTTAGGGTTAGGGC*T	<b>T1</b>
	3' - CTCTTGTCAGTTGTATGTCACAA	<b>T5</b>
<b>TD3</b>	5' - <sup>32</sup> P - GAGAACAGTCAACATACAGTGTAGGGTTAGGGTTAGGGTTAGGGC*T	<b>T1</b>
	3' - CTCTTGTCAGTTGTATGTCACA	<b>T6</b>
<b>T7</b>	5' - GAGAACAGTCAACATACAGTGTTA	

<sup>a</sup>C\* is [<sup>125</sup>I]IdC.

T1+T3 T1 TD1 TD2 TD3

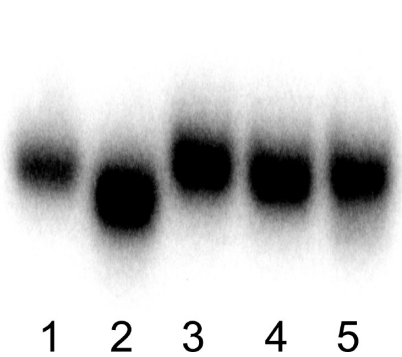


FIGURE 2: Gel-shift assay for formation of the double-stranded complex. Autoradiograph of a native 6% PAGE gel run at room temperature in 1× TBE: lane 1, telomeric oligonucleotide T1 with complementary template T3; lane 2, telomeric oligonucleotide T1; and lanes 3–5, telomeric duplexes TD1, TD2, and TD3, respectively.

and the oligonucleotide was precipitated with ethanol. The pellet was washed with 70% ethanol, vacuum-dried, and dissolved in water.

**Preparation of G-4 Quadruplexes and Radioprob- ing.** The telomeric oligonucleotide labeled with <sup>125</sup>I and <sup>32</sup>P (1 pmol) was annealed with complementary T4, T5, and T6 oligonucleotides (1 pmol) in 44 mM Tris-HCl buffer (pH 7.4). Neither NaCl nor KCl was added at this point because we noticed that the presence of salt prevents complete annealing of the complementary oligonucleotides. Annealing was tested by a band-shift assay in a 4 to 20% gradient precast TBE PAGE gel (Invitrogen, Carlsbad, CA). After the sample had been annealed, NaCl and KCl were added to the samples to a final concentration 100 mM. The samples were incubated for 1 h at 22 °C, flash-frozen in liquid nitrogen, and stored at –80 °C for DNA break accumulation. After 30 days, the samples were thawed, and the integrity of the duplexes was tested once again in a 4 to 20% gradient precast TBE PAGE gel. Strand breaks in the telomeric oligonucleotide were analyzed via 12% denaturing PAGE. Probabilities of breaks were calculated on the basis of the measurement of the

intensity of the bands by densitometry and peak deconvolution as described in detail in ref 15.

**CD Spectroscopy.** CD spectra were recorded on a Jasco J-810 spectropolarimeter in a 2 mm path length cuvette and a wavelength scanning speed of 100 nm/min. The spectra are the averages of three scans between 200 and 320 nm at 25 °C. Telomeric oligonucleotide samples were prepared substantially in the same way that they were for the radioprob- ing assay: 200 μL of a 2 μM solution of oligonucleotide T1 (not labeled with any radioisotope) was annealed in 20 mM sodium or potassium phosphate (pH 7.4) with complementary oligonucleotides (2 μM) to yield TD1, TD2, and TD3 duplexes. After the sample had been annealed, NaCl and KCl were added to the samples to a final concentration 100 mM (Na<sup>+</sup> or K<sup>+</sup>), and samples were incubated for 1 h at 22 °C. All spectra were baseline subtracted, and curves were smoothed using a three-point moving average. Spectra of TD1–TD3 complexes were additionally corrected by subtraction of spectra of the corresponding short duplexes.

**Calculation of Distances.** Interatomic distances were calculated using the coordinates from Protein Data Bank (PDB) entries 143D (7), 1KF1 (8), 2GKU (10), and 2JPZ (20). Guanine cores of the structures were aligned using the MatchMaker function of UCSF Chimera (21), except 143D which was aligned manually. Distances to the guanines of the aligned structures were measured from O4 of residue T25 of the 2JPZ structure.

RESULTS

**Gel-Shift Assay: Demonstration of Formation of the Double-Stranded Complex.** Oligonucleotides TD1, TD2, and TD3, containing 5' duplex and 3' telomeric overhangs, are listed in Table 1. They are different in the length of the duplex region; in TD1, it covers the first TTA triad of the first telomeric repeat, while in TD3, it is two nucleotides shorter and extends only to the first T on the TTA triad (underlined in Table 1). To obtain TD1, TD2, and TD3, the 5'-<sup>32</sup>P, and <sup>125</sup>I-labeled T1 (Table 1) was annealed with 5' complementary oligonucleotides. We noticed that annealing was not 100% (data not shown) if it was conducted in the presence of 100 mM KCl or NaCl, probably

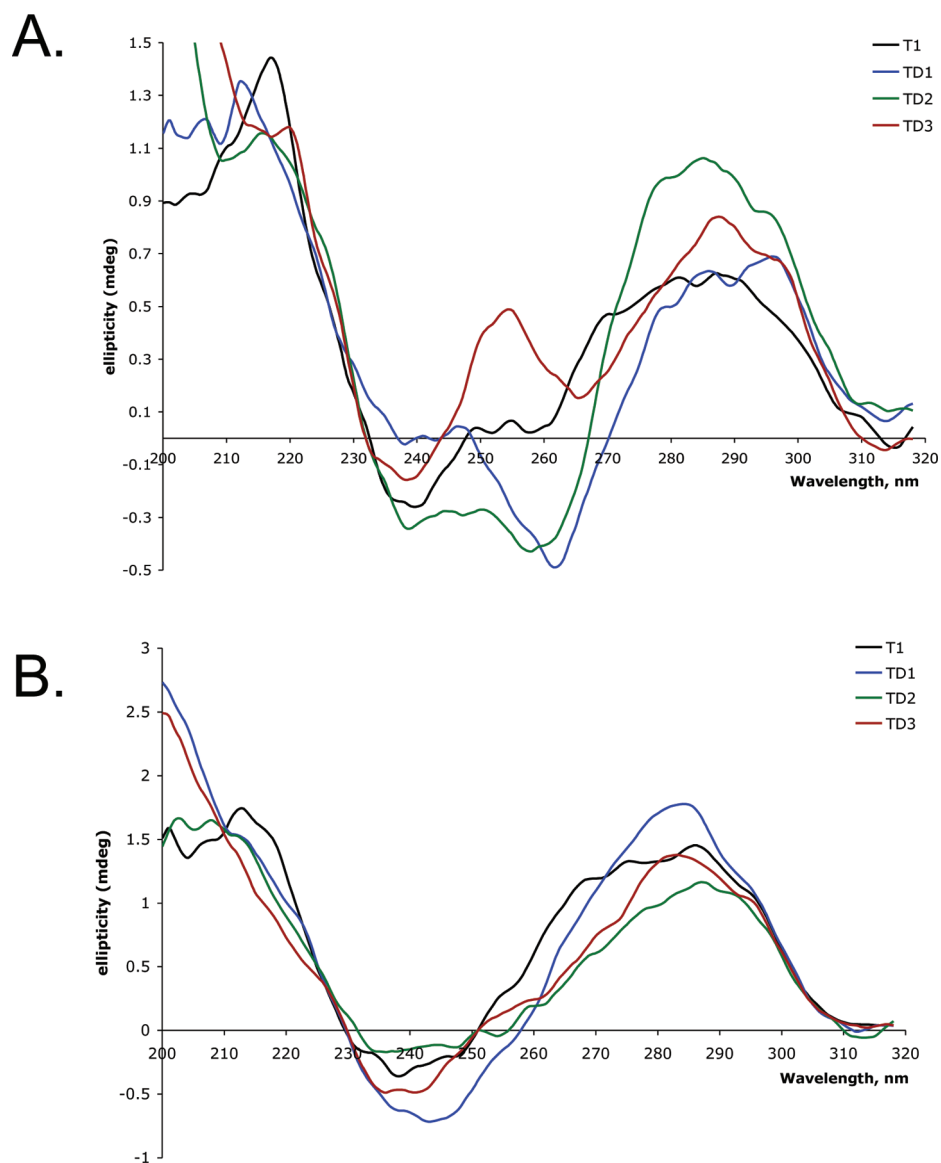


FIGURE 3: Duplex-subtracted CD spectra of telomeric oligonucleotide **T1** and complexes **TD1**, **TD2**, and **TD3** measured in 100 mM Na<sup>+</sup> (A) or 100 mM K<sup>+</sup> (B) at 25 °C.

due to the interaction of the single-stranded 5' end of **T1** with the G-quadruplex structure at the 3' end (14). Therefore, the annealing was conducted in Tris-HCl buffer followed by addition of KCl or NaCl to allow G-quadruplex formation in the 3' overhang under the specified conditions. The extent of annealing was verified by the gel-shift assay (Figure 2). Results shown in Figure 2 demonstrate formation of a duplex between the 5' complementary oligonucleotides **T4**, **T5**, and **T6** and the complementary portion of **T1**. The mobility of **TD1**, **TD2**, and **TD3** duplexes (lanes 3–5) is slower than that of the single-stranded **T1** (lane 2) and comparable with the mobility of the long **T1–T3** duplex (lane 1), thus confirming almost complete formation of the desired DNA constructs.

**CD Spectroscopy Profiles.** We first applied the analysis of circular dichroism (CD) spectra to determine the general type of G-quadruplex conformation in our DNA constructs. CD spectroscopy has been widely used for the characterization of G-quadruplex-forming oligonucleotides (9, 22–28). CD spectra are generally affected by the orientation of guanine residues relative to the sugar moieties, i.e., anti or syn, and by sugar pucker. Therefore, antiparallel and mixed-type quadruplexes

containing both anti and syn conformations of guanines and parallel quadruplexes with all guanines in the anti conformation can be distinguished by their CD spectra. Nucleotides of the loops, and that in the 5' and 3' extensions, also contribute to CD spectra, complicating their interpretation. In strict terms, it is impossible to predict the exact fold of a quadruplex solely on the basis of its CD spectra. Nevertheless, reference spectra have been determined for different G-quadruplex conformations. Thus, CD spectra of antiparallel basket and chair conformations of telomeric DNA have a characteristic strong positive peak at 295 nm, a smaller negative peak at 265 nm, and a positive peak at 245 nm (29). Mixed 3+1 conformations exhibit a strong peak at 290 nm, a shoulder peak at 268 nm, and a negative peak at 240 nm (9). CD spectra of the parallel conformation of telomeric DNA are expected to have a positive peak near 260 nm and a negative peak near 240 nm, based on the spectra of short G-rich telomeric oligonucleotides that formed tetramolecular parallel structures (29). Intramolecular structures with such CD spectra were described as parallel quadruplexes (25, 27); however, the parallel fold of these intramolecular quadruplexes has not been confirmed by other methods in solution. Also, on the basis of CD



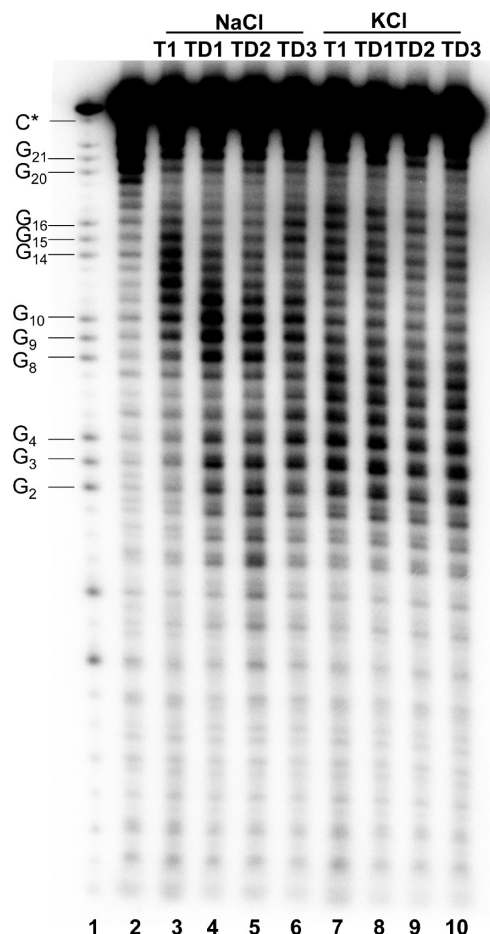


FIGURE 4: Analysis of DNA breaks in telomeric oligonucleotides by 12% denaturing PAGE: lane 1, G sequencing ladder; lane 2, duplex of **T1** with complementary template **T3**; lanes 3–6, oligonucleotide **T1** and complexes **TD1**, **TD2**, and **TD3**, respectively, folded in a 100 mM NaCl solution; and lanes 7–10, oligonucleotide **T1** and complexes **TD1**, **TD2**, and **TD3**, respectively, folded in a 100 mM KCl solution.

spectra of the GGGTTAGGG oligonucleotide forming a dimeric all-parallel quadruplex, a positive band at 290 nm was assigned to the contribution of external loop residues (25).

The duplex regions of **TD1**, **TD2**, and **TD3** significantly contribute to the overall CD spectra of these molecules. To extract these contributions, oligonucleotides forming just the duplex parts of **TD1**, **TD2**, and **TD3** were synthesized and annealed, and their CD spectra were subtracted from the overall spectra of **TD1**, **TD2**, and **TD3**. CD spectra of **T1**, and the “duplex-subtracted” spectra of **TD1**, **TD2**, and **TD3** in the presence of  $\text{Na}^+$  or  $\text{K}^+$ , are shown in Figure 3. The raw CD spectra before subtraction are available as Supporting Information (Figure S1).

In the presence of  $\text{Na}^+$ , CD spectra are clearly affected by the formation of the duplex at the 5' end of **T1**. The spectra of **TD1**, **TD2**, and **TD3** are quite different from that of **T1**. At the same time, while CD spectra of **TD1** and **TD2** are similar to each other they are completely different from the CD spectrum of **TD3** that exhibits a strong positive peak at  $\sim 255$  nm. The CD spectrum of **T1** with a positive peak at 290 nm, a shoulder peak at 268 nm, and a negative peak at 240 nm is consistent with the signature of a mixed 3+1 quadruplex conformation. The CD spectrum of **TD1** shows general features of an antiparallel quadruplex, a positive peak at 295 nm and a negative around 260 nm, but the lack of a

positive peak at 240 nm and a positive peak at 280 nm indicates the presence of other quadruplex conformations. The CD spectrum of **TD2** does not correspond to a single quadruplex conformation and can be interpreted as a spectrum of a mixture of antiparallel and mixed conformations. **TD3** is the only conformation that has a distinct positive peak at 255 nm; that, along with the negative peak at 240 nm, is consistent with the presence of the parallel quadruplex conformation.

In the presence of  $\text{K}^+$ , CD spectra of all tested complexes (Figure 3B) are consistent with the signature of a mixed 3 + 1 quadruplex conformation. With slight variations, they all have a maximum at  $\sim 285$ – $295$  nm, a shoulder between 260 and 270 nm, and a minimum at  $\sim 240$ – $245$  nm.

**Radioprobings of Telomeric Quadruplexes.** To assess the exact fold of intramolecular quadruplexes in **TD1**, **TD2**, and **TD3**, we applied  $^{125}\text{I}$  radioprobings. **TD1**, **TD2**, and **TD3** were allowed to fold under the specified conditions, and then samples were frozen in liquid nitrogen and stored for 2 weeks for the accumulation of  $^{125}\text{I}$ -induced DNA strand breaks. Then the samples were analyzed for strand breaks by sequencing PAGE (Figure 4). Figure 5 shows the probabilities of breaks at the individual nucleotides based on the measurement of the intensity of the bands by densitometry and peak deconvolution (for details, see ref 15).

For analysis of the radioprobings results, we used the same considerations and rules that we described in our previous paper (15). We focused our attention on guanines in the core of the G-quadruplex. We showed that the geometry of the cores is very similar for all quadruplex conformations, disregarding, of course, the fact that different guanines are in different positions in these conformations. Our interpretation of radioprobings data was based on a simple geometric consideration; if  $^{125}\text{I}$  is at the “bottom” of the core, then the guanines at the “top” of the core are the most distant from it and, consequently, would have the lowest probability of breaks. To prove this, we calculated distances from O4 of the 3' T25 located at the bottom of the 3+1 type 2 NMR structure [PDB entry 2JPZ (20)] to the sugars of the core guanines. In addition, using UCSF Chimera (21), we align cores of other quadruplexes [PDB entries 1KF1, 143D, and 2GKU (7, 8, 10)] with that of 2JPZ. Then we measured distances from O4 of T25 of 2JPZ to the sugars of guanines of the other aligned structures. The results are presented in Figure 6. As expected, for all tested quadruplex conformations, the distances increase as we move from the position in the bottom of the core to the top (as they are oriented in Figure 1). Therefore, if the probability of breaks decreases along a run of three guanines, then it means that the distance increases from the first to the last guanine in the run. If “↑” indicates the increase in distances and “↓” the decrease, then, for example, the basket conformation can be described as G22↑G20, G16↓G14, G10↑G8, G4↓G2, “3+1” type 1 as G22↑G20, G16↓G14, G10↑G8, G4↑G2, and propeller as G22↑G20, G16↑G14, G10↑G8, G4↑G2. Obviously, the distances always increase along the G22–G20 side; therefore, we will omit it in our descriptions.

**Conformation of TD Complexes in  $\text{Na}^+$ .** Figure 5A shows the results of the radioprobings experiment with single-stranded **T1** and **TD1**, **TD2**, and **TD3** complexes in the presence of  $\text{Na}^+$ . The higher the probability of breaks, the closer the nucleotide to the  $^{125}\text{I}$ -dC at the 3' end of the structure. Accordingly, for **T1**, the decrease in the likelihood of breaks from G14 to G16 shows that the former is closer to the bottom of the structure than the latter. Likewise, G10 is closer than G8. The probabilities of breaks are

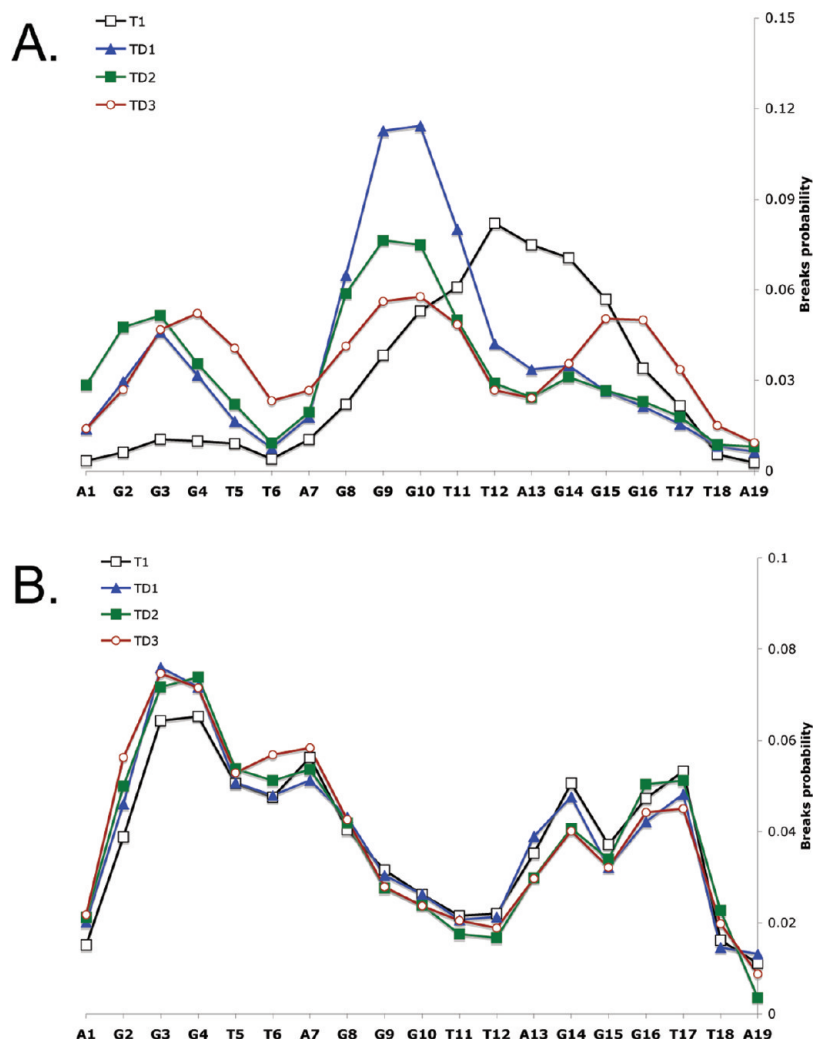


FIGURE 5: Distribution of  $^{125}\text{I}$ -induced strand break probability in the telomeric oligonucleotide **T1** and complexes **TD1**, **TD2**, and **TD3** in 100 mM NaCl (A) or 100 mM KCl (B).

the lowest for the G2–G4 side, indicating that it is diagonal to the G22 position. Overall, the distribution of breaks for **T1** in  $\text{Na}^+$  can be described as G16↓G14, G10↑G8, G4↑G2.

Duplex formation at the 5' end of **T1** (**TD1**, **TD2**, and **TD3**) drastically changes the distributions of breaks. For **TD3**, there is a clear pattern of an increase in the likelihood of breaks along all G-sides. The structure can be described as G22↑G20, G16↑G14, G10↑G8, G4↑G2 and corresponds to all-parallel propeller conformation of quadruplex, consistent with the CD spectra. For **TD1** and **TD2**, distributions of breaks are similar to each other; both have a pronounced maximum at G10 and G9. The **TD1** conformation can be formally described as G16↓G14, G10↑G8, G4↑G2 and that of **TD2** as G16↓G14, G10↑G8, G4↑G2, where “↑” indicates the lack of a clear increase or decrease in break probability along G2–G4 and G8–G10 sides. This uncertainty does not allow us to unambiguously ascribe the observed distribution of breaks to any single G-quadruplex conformation. Therefore, we conclude that in  $\text{Na}^+$  **TD1** and **TD2** are present as a mixture of different isomers of G-quadruplex. This conclusion is in accord with the CD spectroscopy data (Figure 3).

**Conformation of TD Complexes in  $\text{K}^+$ .** Figure 5B shows the results of a radioprobe experiment of **T1**, **TD1**, **TD2**, and **TD3** complexes in the presence of KCl. In contrast to the NaCl data and in agreement with CD spectra, there is no significant difference in the distribution of break probabilities among all

tested oligonucleotides. Probabilities of breaks are almost the same for G16 and G14. They are lowest for G8–G10, with a weak increase in break probabilities along the G8–G10 side. At the same time, there is a clear decrease in break probability for G4–G2 and the nucleotides at the 5' end from them indicating that this side and the 5' region are moving away from the  $^{125}\text{I}$  that is at the 3' end (bottom of Figure 1) of the molecules. Quadruplex conformations can be formally described as G16↓G14, G10↓G8, G4↓G2, where ↓ indicates the lack of a clear increase or decrease in break probability along the G16–G14 side. As in our previous study, in the presence of  $\text{K}^+$  (15), it is impossible to clearly attribute this break distribution to a single G-quadruplex conformation. Hence, the radioprobe results point to a mixture of quadruplex conformations in the presence of  $\text{K}^+$  for all tested oligonucleotides.

## DISCUSSION

The simultaneous presence of several quadruplex conformations in solution poses a challenge to any structural method and complicates interpretation of experimental results. Next we will try to deduce structural information from the results of our radioprobe experiments in light of our CD spectra. CD spectra indicate that in  $\text{K}^+$  the quadruplexes are in a mixed 3+1 conformation. From the NMR studies (9, 10, 20, 30), we know

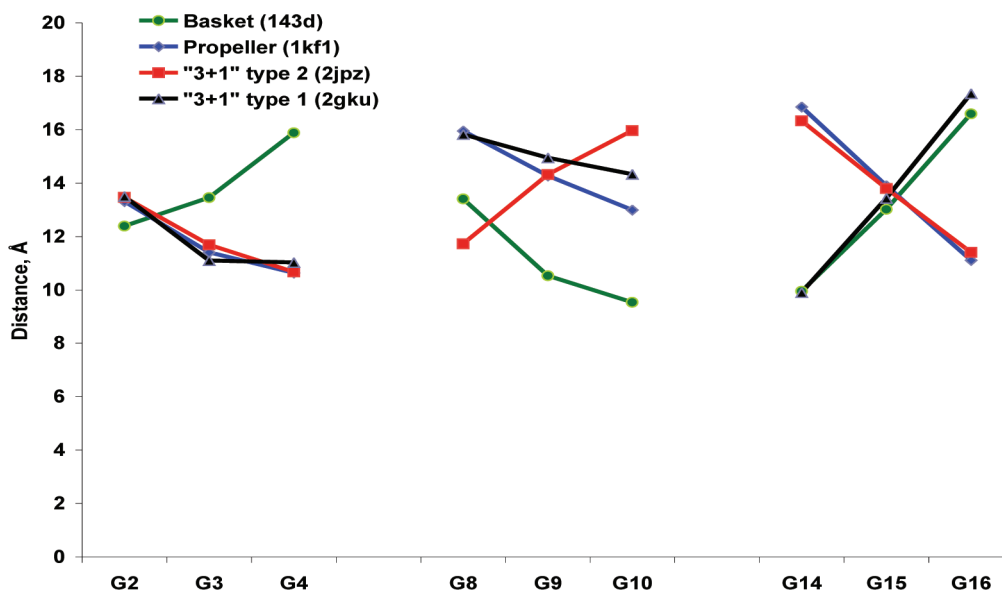


FIGURE 6: Average distances (in angstroms) from O4 of T25 of the quadruplex structure from PDB entry 2JPZ to the sugars of the guanines in the core of 2JPZ and three other quadruplex conformations from PDB entries 1KF1, 143D, and 2GKU that were aligned with 2JPZ as described in Materials and Methods. Different conformations of the G-quadruplex: green, basket, PDB entry 143D; blue, propeller, PDB entry 1KF1; red, 3+1 type 2, PDB entry 2JPZ; and black, 3+1 type 1, PDB entry 2GKU.

that telomeric oligonucleotides in the presence of  $K^+$  can adopt two isomers of mixed 3+1 conformation, type 1 and type 2 (Figure 1). The main ambiguity in our radioprobings data in  $K^+$  (Figure 5B) is the lack of an increase or a decrease in break probability along G16–G14 side. We believe that this ambiguity is consistent with the presence of the mixture of type 1 and type 2 isomers of mixed 3+1 conformation. Indeed, in type 1 and type 2 isomers (Figure 1), the G16–G14 side points in different directions; therefore, in the type 1 isomer, the maximum probability of breaks along this side is at G14, while in the type 2 isomer, it is at G16. Superposition of these two distributions would result in the pattern of breaks observed in Figure 5B, i.e., equal at G14 and G16 and somewhat lower at G15. Guanines along the G10–G8 side have the lowest break probability, consistent with this side being diagonal (i.e., most distant) from the  $^{125}I$  position in both type 1 and type 2 isomers of mixed 3+1 conformation. Although the G10–G8 side is in different orientations in type 1 and type 2 isomers, we observe steady decrease in break probability from G8 to G10. This discrepancy could be due, for example, to the nonlinear relation between the distance and probability of breaks. Thus, in the type 2 isomer, the distance from G8 to  $^{125}I$  is considerably shorter than the distance from G10 to  $^{125}I$  in the type 1 isomer (Figure 6). This could explain why the overall break probability at G8 is higher than that at G10 in the mixture of the isomers.

The distribution of breaks for **T1** in  $Na^+$  was G16/G14, G10/G8, G4/G2. This distribution is consistent with both type 1 and basket mixed 3+1 conformations (Figure 1). The probabilities of breaks are the lowest for the G2–G4 side, indicating that it is the most distant from (i.e., diagonal to) the  $^{125}I$  position. Therefore, **T1** is most likely in the mixed 3+1 basket conformation that we proposed in our previous study for a similar telomeric oligonucleotide with a 5' extension (15). The CD spectrum of **T1** in  $Na^+$  is also consistent with a mixed 3+1 conformation.

CD spectra of **TD1** and **TD2** in  $Na^+$  exhibited certain features of both antiparallel and 3+1 conformations. The main ambiguity in their radioprobings profiles (Figure 5A, blue and green curves)

is the lack of any clear increase or decrease in break probability along the G4–G2 side. This is consistent with a mixture of the antiparallel basket and 3+1 basket conformations. In these two conformations, only the G4–G2 side points in different directions relative to the  $^{125}I$  position. In the antiparallel basket, G2 is the closest to  $^{125}I$ , while in the 3+1 basket, it is G4. Superposition of the break distributions characteristic of these two basket conformations is consistent with that observed for **TD1** and **TD2**. The difference in the break distributions for **TD1** and **TD2** could be attributed to various proportions of these conformers in the mixtures.

The considerations mentioned above define major quadruplex conformations present simultaneously in  $K^+$  and  $Na^+$  solutions, i.e., 3+1 type 1 and type 2 for all studied molecules in  $K^+$  and antiparallel and 3+1 basket for **TD1** and **TD2** in  $Na^+$ . However, not all the features of break distribution profiles can be explained by these considerations. For example, we cannot explain a considerably higher break probability at G10 and G9 compared to that at G14 and G15 for **TD1** in  $Na^+$ . As we previously discussed (15), radioprobings (i.e., distribution of DNA break probability), in principle, should provide accurate information about internal distances in a DNA molecule. However, in the labeling scheme used in our study, the exact position of the  $^{125}I$  was not fixed, thus causing some degree of uncertainty in the interpretation of the results.

We should note here that the order of the distances to the sugars of the core guanines depends considerably on the position of the  $^{125}I$  at the bottom of the core. For example, the distance from C1' of G22 that is in the corner of the core to G2 at the top is actually shorter than that to G4 at the bottom of the core (Figure 2 of ref 15). Therefore, in our previous paper (15), interpretation of radioprobings data was actually based on simple geometrical considerations rather than on the actual distances. The distances were presented to prove that the cores of all quadruplexes had similar geometries, and G22 was chosen simply because the "extra core" nucleotides are different in different structures (some of the structures do not have extra nucleotides at the 3' end at all). Herein, by aligning cores of different G-quadruplexes,



we actually showed that the distances from a reference position at the bottom of the core follow the predicted pattern; i.e., guanines at the top of the core are more distant than at the bottom. At the same time, we noticed that if the reference position was moved to the periphery of the core and closer to the G-tetrad at the bottom the order of the guanines in terms of distances could be altered (I. G. Panyutin, unpublished observation), like it was in the extreme case of the C1' position of G22 (see above). Therefore, formation of the duplex at the 5' end of the molecules could affect the position of the  $^{125}\text{I}$ -dC, especially in antiparallel conformations driving it closer to one G-side or another. This could be an alternative to the explanation presented above for the ambiguities in radioprobe data observed for **TD1** and **TD2** in  $\text{Na}^+$ . At the same time, we could not exclude a minor presence of other quadruplex conformations in solutions that would affect fine details of break distribution profiles.

Nevertheless, the combination of radioprobe data and CD spectra strongly indicates the presence of an all-parallel propeller quadruplex conformation in **TD3** in  $\text{Na}^+$ . This quadruplex conformation of telomeric DNA was first observed by X-ray crystallography. There were also several reports describing this conformation in some special conditions in solution (25, 31). It is possible that folding of telomeric overhangs into this conformation requires stabilizing interactions with similar neighboring quadruplexes as in crystal (8) or in the case of multiple telomeric repeats (27). In our study, the duplex region could provide such stabilization. Thus, folding of the first (from the duplex) four repeats into the parallel quadruplex may trigger folding of the rest of the repeats in the single-stranded overhang into the same conformation. This would result in contraction of the overhangs normally prevented by telomeric proteins such as POT1 and may play a role in the functioning of telomeres, which was previously discussed (8).

Recently, a new basket conformation of the telomeric quadruplex stabilized by two G-tetrads was described by NMR in  $\text{K}^+$  (16). The CD spectrum of this conformation is somewhat similar to that observed in our study for **TD3** in  $\text{Na}^+$  (Figure 2A). However, our radioprobe data for **TD3** are inconsistent with the presence of this conformation. For example, in this new basket conformation, G14 would be the closest to  $^{125}\text{I}$  at the 3' end, while the radioprobe profile (Figure 5A) shows that G16 is the closest to  $^{125}\text{I}$ . Radioprobe profiles of other molecules described here do not support the presence of this new basket conformation either. Nevertheless, as discussed above, we cannot exclude a minor presence of this form of the quadruplex.

Previous studies utilizing NMR and X-ray crystallography methods determined molecular structures of telomeric quadruplexes in single-stranded G-rich oligonucleotides, laying down a framework for further structure–function relation studies in telomeric DNA. Their application to more realistic models of telomeres containing multiple repeats in both single- and double-stranded form is currently complicated by the size of such DNA molecules. In our study, by combining radioprobe and CD spectroscopy, we were able to gain detailed information regarding the conformation of telomeric quadruplexes in DNA molecules containing both duplex and quadruplex domains. We showed that in the presence of  $\text{Na}^+$  one of these molecules adopts the all-parallel propeller quadruplex conformation. We also concluded that in  $\text{Na}^+$  two other molecules were present as a mixture of antiparallel and 3+1 basket conformations while in  $\text{K}^+$  all the molecules were present as a mixture of 3+1 type 1 and type 2 conformations.

## ACKNOWLEDGMENT

We thank Dr. P. Schuck for the help with CD measurements.

## SUPPORTING INFORMATION AVAILABLE

Raw CD spectra of reference duplexes and complexes. This material is available free of charge via the Internet at <http://pubs.acs.org>.

## REFERENCES

1. Moyzis, R. K., Buckingham, J. M., Cram, L. S., Dani, M., Deaven, L. L., Jones, M. D., Meyne, J., Ratliff, R. L., and Wu, J. R. (1988) A highly conserved repetitive DNA sequence,  $(\text{TTAGGG})_n$ , present at the telomeres of human chromosomes. *Proc. Natl. Acad. Sci. U.S.A.* 85, 6622–6626.
2. Sfeir, A. J., Chai, W., Shay, J. W., and Wright, W. E. (2005) Telomere-end processing the terminal nucleotides of human chromosomes. *Mol. Cell* 18, 131–138.
3. Gellert, M., Lipsett, M. N., and Davies, D. R. (1962) Helix Formation by Guanylic Acid. *Proc. Natl. Acad. Sci. U.S.A.* 48, 2013–2018.
4. Sen, D., and Gilbert, W. (1988) Formation of parallel four-stranded complexes by guanine-rich motifs in DNA and its implications for meiosis. *Nature* 334, 364–366.
5. Williamson, J. R., Raghuraman, M. K., and Cech, T. R. (1989) Monovalent cation-induced structure of telomeric DNA: The G-quartet model. *Cell* 59, 871–880.
6. Panyutin, I. G., Kovalsky, O. I., Budowsky, E. I., Dickerson, R. E., Rikhirev, M. E., and Lipanov, A. A. (1990) G-DNA: A twice-folded DNA structure adopted by single-stranded oligo(dG) and its implications for telomeres. *Proc. Natl. Acad. Sci. U.S.A.* 87, 867–870.
7. Wang, Y., and Patel, D. J. (1993) Solution structure of the human telomeric repeat  $d[\text{AG}_3(\text{T}_2\text{AG}_3)_3]$  G-tetraplex. *Structure* 1, 263–282.
8. Parkinson, G. N., Lee, M. P., and Neidle, S. (2002) Crystal structure of parallel quadruplexes from human telomeric DNA. *Nature* 417, 876–880.
9. Ambrus, A., Chen, D., Dai, J., Bialis, T., Jones, R. A., and Yang, D. (2006) Human telomeric sequence forms a hybrid-type intramolecular G-quadruplex structure with mixed parallel/antiparallel strands in potassium solution. *Nucleic Acids Res.* 34, 2723–2735.
10. Luu, K. N., Phan, A. T., Kuryavyi, V., Lacroix, L., and Patel, D. J. (2006) Structure of the human telomere in  $\text{K}^+$  solution: An intramolecular (3+1) G-quadruplex scaffold. *J. Am. Chem. Soc.* 128, 9963–9970.
11. He, Y., Neumann, R. D., and Panyutin, I. G. (2004) Intramolecular quadruplex conformation of human telomeric DNA assessed with  $^{125}\text{I}$ -radioprobe. *Nucleic Acids Res.* 32, 5359–5367.
12. Włodarczyk, A., Grzybowski, P., Patkowski, A., and Dobek, A. (2005) Effect of ions on the polymorphism, effective charge, and stability of human telomeric DNA. Photon correlation spectroscopy and circular dichroism studies. *J. Phys. Chem. B* 109, 3594–3605.
13. Redon, S., Bombard, S., Elizondo-Riojas, M. A., and Chottard, J. C. (2003) Platinum cross-linking of adenines and guanines on the quadruplex structures of the  $\text{AG}_3(\text{T}_2\text{AG}_3)_3$  and  $(\text{T}_2\text{AG}_3)_4$  human telomere sequences in  $\text{Na}^+$  and  $\text{K}^+$  solutions. *Nucleic Acids Res.* 31, 1605–1613.
14. Dai, J., Punchihewa, C., Ambrus, A., Chen, D., Jones, R. A., and Yang, D. (2007) Structure of the intramolecular human telomeric G-quadruplex in potassium solution: A novel adenine triple formation. *Nucleic Acids Res.* 35, 2440–2450.
15. Gaynutdinov, T. I., Neumann, R. D., and Panyutin, I. G. (2008) Structural polymorphism of intramolecular quadruplex of human telomeric DNA: Effect of cations, quadruplex-binding drugs and flanking sequences. *Nucleic Acids Res.* 36, 4079–4087.
16. Lim, K. W., Amrane, S., Bouaziz, S., Xu, W., Mu, Y., Patel, D. J., Luu, K. N., and Phan, A. T. (2009) Structure of the human telomere in  $\text{K}^+$  solution: A stable basket-type G-quadruplex with only two G-tetrad layers. *J. Am. Chem. Soc.* 131, 4301–4309.
17. Neidle, S., and Parkinson, G. N. (2008) Quadruplex DNA crystal structures and drug design. *Biochimie* 90, 1184–1196.
18. Rezler, E. M., Bearss, D. J., and Hurley, L. H. (2003) Telomere inhibition and telomere disruption as processes for drug targeting. *Annu. Rev. Pharmacol. Toxicol.* 43, 359–379.
19. Panyutin, I. G., and Neumann, R. D. (1997) Radioprobe of DNA: Distribution of DNA breaks produced by decay of  $^{125}\text{I}$  incorporated into a triplex-forming oligonucleotide correlates with geometry of the triplex. *Nucleic Acids Res.* 25, 883–887.



20. Dai, J., Carver, M., Punchihewa, C., Jones, R. A., and Yang, D. (2007) Structure of the hybrid-2 type intramolecular human telomeric G-quadruplex in  $K^+$  solution: Insights into structure polymorphism of the human telomeric sequence. *Nucleic Acids Res.* 35, 4927–4940.
21. Pettersen, E. F., Goddard, T. D., Huang, C. C., Couch, G. S., Greenblatt, D. M., Meng, E. C., and Ferrin, T. E. (2004) UCSF Chimera: A visualization system for exploratory research and analysis. *J. Comput. Chem.* 25, 1605–1612.
22. Rezler, E. M., Seenisamy, J., Bashyam, S., Kim, M. Y., White, E., Wilson, W. D., and Hurley, L. H. (2005) Telomestatin and diseleno saphyrin bind selectively to two different forms of the human telomeric G-quadruplex structure. *J. Am. Chem. Soc.* 127, 9439–9447.
23. Giraldo, R., Suzuki, M., Chapman, L., and Rhodes, D. (1994) Promotion of parallel DNA quadruplexes by a yeast telomere binding protein: A circular dichroism study. *Proc. Natl. Acad. Sci. U.S.A.* 91, 7658–7662.
24. Hardin, C. C., Watson, T., Corregan, M., and Bailey, C. (1992) Cation-dependent transition between the quadruplex and Watson-Crick hairpin forms of d(CGCG<sub>3</sub>GCG). *Biochemistry* 31, 833–841.
25. Rujan, I. N., Meleney, J. C., and Bolton, P. H. (2005) Vertebrate telomere repeat DNAs favor external loop propeller quadruplex structures in the presence of high concentrations of potassium. *Nucleic Acids Res.* 33, 2022–2031.
26. Gray, R. D., Li, J., and Chaires, J. B. (2009) Energetics and Kinetics of a Conformational Switch in G-Quadruplex DNA. *J. Phys. Chem. B* 113, 2676–2683.
27. Vorlickova, M., Chladkova, J., Kejnovska, I., Fialova, M., and Kypr, J. (2005) Guanine tetraplex topology of human telomere DNA is governed by the number of (TTAGGG) repeats. *Nucleic Acids Res.* 33, 5851–5860.
28. Kypr, J., Kejnovska, I., Rencuk, D., and Vorlickova, M. (2009) Circular dichroism and conformational polymorphism of DNA. *Nucleic Acids Res.* 37, 1713–1725.
29. Dapic, V., Abdomerovic, V., Marrington, R., Peberdy, J., Rodger, A., Trent, J. O., and Bates, P. J. (2003) Biophysical and biological properties of quadruplex oligodeoxyribonucleotides. *Nucleic Acids Res.* 31, 2097–2107.
30. Phan, A. T., Luu, K. N., and Patel, D. J. (2006) Different loop arrangements of intramolecular human telomeric (3+1) G-quadruplexes in  $K^+$  solution. *Nucleic Acids Res.* 34, 5715–5719.
31. Xue, Y., Kan, Z. Y., Wang, Q., Yao, Y., Liu, J., Hao, Y. H., and Tan, Z. (2007) Human telomeric DNA forms parallel-stranded intramolecular G-quadruplex in  $K^+$  solution under molecular crowding condition. *J. Am. Chem. Soc.* 129, 11185–11191.